



OPEN

A radio technosignature search towards Proxima Centauri resulting in a signal of interest

Shane Smith^{1,2}, Danny C. Price^{1,2,3}✉, Sofia Z. Sheikh^{1,2}, Daniel J. Czech², Steve Croft^{2,4}, David DeBoer^{1,5}, Vishal Gajjar², Howard Isaacson^{1,6}, Brian C. Lacki², Matt Lebofsky^{1,2}, David H. E. MacMahon⁵, Cherry Ng^{2,4,7}, Karen I. Perez⁸, Andrew P. V. Siemion^{2,4,9}, Claire Isabel Webb^{2,10}, Jamie Drew¹¹, S. Pete Worden¹¹ and Andrew Zic^{12,13}

The detection of life beyond Earth is an ongoing scientific pursuit, with profound implications. One approach, known as the search for extraterrestrial intelligence (SETI), seeks to find engineered signals ('technosignatures') that indicate the existence of technologically capable life beyond Earth. Here, we report on the detection of a narrowband signal of interest at ~982 MHz, recorded during observations towards Proxima Centauri with the Parkes Murriyang radio telescope. This signal, BLC1, has characteristics broadly consistent with hypothesized technosignatures and is one of the most compelling candidates to date. Analysis of BLC1—which we ultimately attribute to being an unusual but locally generated form of interference—is provided in a companion paper. Nevertheless, our observations of Proxima Centauri are a particularly sensitive search for radio technosignatures towards a stellar target.

The discovery of the exoplanet Proxima Centauri b (Prox Cen b) in orbit around Prox Cen¹ has sparked excitement over the prospect of a habitable exoplanet in the nearest reaches of the solar neighbourhood. Several studies^{2–4} suggest that Prox Cen b may be able to sustain an atmosphere favourable for life. However, because Prox Cen is an active M-dwarf flare star, doubt has been cast on the ability of Prox Cen b, which is in a much tighter orbit than Earth is to the Sun, to retain an atmosphere amenable to the existence of biological life. A naked-eye visible superflare strong enough to kill any known organisms has been observed from Prox Cen⁵, although life could still exist on the cold side of a tidally locked planet. Coronal mass ejections from Prox Cen have also been observed^{6,7}, suggesting that Prox Cen b experiences appreciable ionizing radiation. Nevertheless, there remain compelling arguments that M-dwarf stars are viable hosts for life-bearing planets⁸, and Prox Cen b remains a compelling target for biosignature and technosignature searches.

Prox Cen b is also a candidate for in situ searches for extraterrestrial life by Breakthrough Starshot⁹. Starshot seeks to launch a gram-sized spacecraft propelled using a laser light sail at a relativistic velocity (0.2c) to the Alpha Centauri system with Prox Cen b as the primary target. If successful, the spacecraft will travel the 4.22 light yr to Prox Cen in 20 yr and then transmit information on its target(s) back to Earth.

Despite being our nearest stellar neighbour, few technosignature searches have been conducted towards Prox Cen. In the 1990s, two search for extraterrestrial intelligence (SETI) programmes were conducted in the southern hemisphere towards nearby stars: the Project Phoenix search of 202 solar-like stars^{10,11}, and a search for

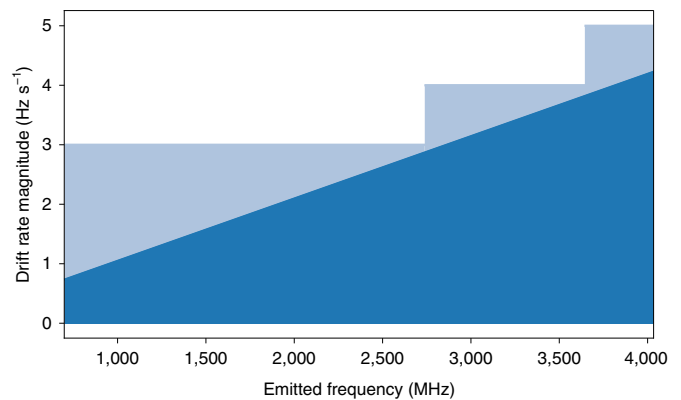


Fig. 1 | Expected Doppler drift from a transmitter located on the surface of Prox Cen b. Dark blue is the calculated magnitude of the Doppler drift and light blue is the magnitude of the search range.

technosignatures from 176 of the brightest stars¹². Consequently, neither programme selected Prox Cen—a faint M dwarf—as a star target. Until a recent technosignature search of high-resolution optical spectra of Prox Cen¹³, no technosignature searches had been conducted at optical wavelengths. This search of archival data from the High Accuracy Radial Velocity Planet Searcher spectrometer between 2004 and 2019 would have revealed laser emission from Prox Cen with <120 kW power, and was motivated by the observations detailed here.

¹Department of Physics, Hillsdale College, MI, Hillsdale, USA. ²Department of Astronomy, University of California Berkeley, CA, Berkeley, USA.

³International Centre for Radio Astronomy Research, Curtin University, Western Australia, Perth, Australia. ⁴SETI Institute, CA, Mountain View, USA.

⁵Radio Astronomy Laboratory, University of California Berkeley, CA, Berkeley, USA. ⁶University of Southern Queensland, Queensland, Toowoomba, Australia.

⁷Dunlap Institute for Astronomy & Astrophysics, University of Toronto, Toronto, Ontario, Canada. ⁸Department of Astronomy, Columbia University, NY, New York, USA.

⁹Department of Physics & Astronomy, University of Manchester, Manchester, UK. ¹⁰Berggruen Institute, CA, Los Angeles, USA.

¹¹Breakthrough Initiatives, CA, Moffett Field, USA. ¹²Department of Physics and Astronomy, and Research Centre in Astronomy, Astrophysics and Astrophotonics, Macquarie University, New South Wales, Sydney, Australia.

¹³Australia Telescope National Facility, CSIRO, Space and Astronomy, New South Wales, Epping, Australia.

✉e-mail: dancpr@berkeley.edu

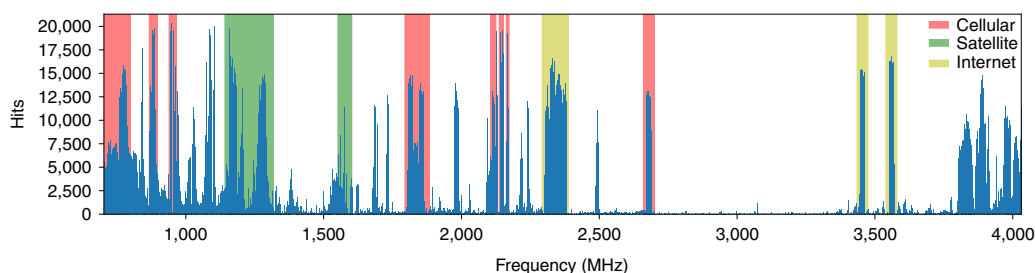


Fig. 2 | A histogram of total hits as a function of frequency (narrowband signals detected above S/N threshold) for our observations towards Prox Cen. We used the turboSETI Doppler search code to search for narrowband signals with a Doppler drift across the 0.7–4.0 GHz bandwidth of the Parkes UWL receiver. Registered cellular, satellite and broadband internet transmitters in the Parkes area are overlaid.

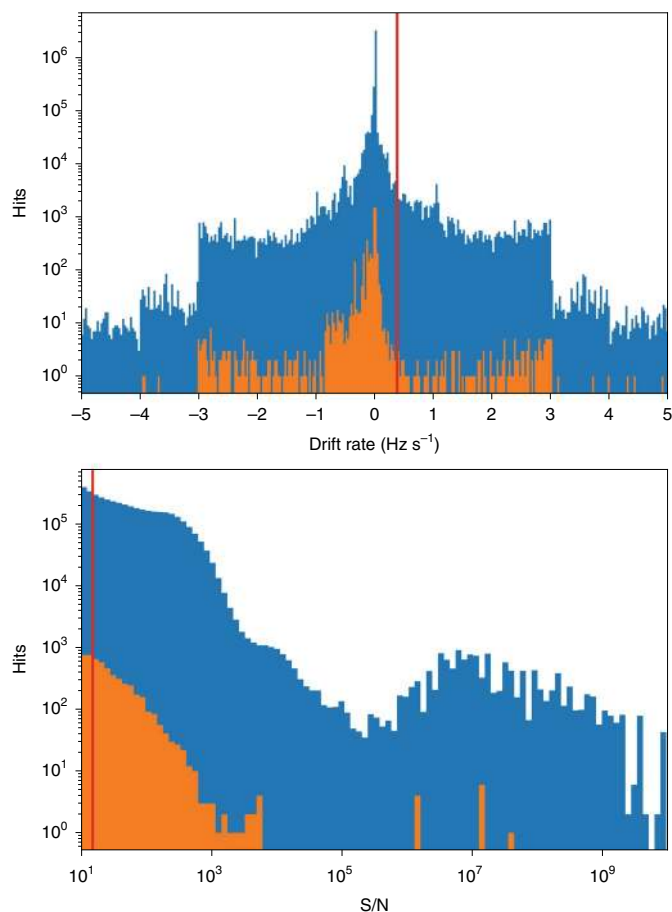


Fig. 3 | Histograms with total hits and events. Search drift rates (top panel) and S/N (bottom panel). Blue bins are hits (signals detected by our data analysis pipeline) and orange bins are events (signals detected in all on-source observations, but not in off-source observations).

In this Article, we present a search for technosignatures from the direction of Prox Cen, using the CSIRO Parkes radio telescope (‘Murriyang’) as part of the Breakthrough Listen (BL) and the Breakthrough Initiatives search for life beyond Earth. BL—a sister initiative of Starshot—is a 10 yr programme to search for signs of intelligent life at radio and optical wavelengths^{14,15}. BL has been conducting observations since 2016 and is undertaking the most rigorous and comprehensive observational SETI campaign to date^{16–20}. Prox Cen is part of the BL survey sample of 60 stars within 5 pc (ref. 15), and was observed as part of a previous data release including 1,327 nearby stars¹⁷. These observations were conducted using the Parkes 10 cm receiver, covering 2.60–3.45 GHz. The observa-

tions presented here cover a larger bandwidth (0.7–4.0 GHz), with six times longer on-source dwell times (30 min). Our observations allow us to set the lowest equivalent isotropic radiated power (EIRP) detection limit for any stellar target.

We searched our observations towards Prox Cen for signs of technologically advanced life, across the full frequency range of the receiver (0.7–4.0 GHz). To search for narrowband technosignatures we exploit the fact that signals from any body with a non-zero radial acceleration relative to Earth, such as an exoplanet, solar system object or spacecraft, will exhibit a characteristic time-dependent drift in frequency (referred to as a drift rate) when detected by a receiver on Earth. We applied a search algorithm that detects narrowband signals with Doppler drift rates consistent with that expected from a transmitter located on the surface of Prox Cen b (Fig. 1). Our search detected a total of 4,172,702 hits—that is, narrowband signals detected above a signal-to-noise (S/N) threshold—in all on-source observations of Prox Cen and reference off-source observations. Of these, 5,160 hits were present in multiple on-source pointings towards Prox Cen, but were not detected in reference (off-source) pointings towards calibrator sources; we refer to these as ‘events’ (Table 1).

The total hits by frequency are shown in Fig. 2. As expected, our detection pipeline finds the majority of hits (57%) in ranges that have registered transmitters. Distributions of hits and events for our drift rate search range and S/N are shown in Fig. 3. Positive, negative and zero drift rates correspond to 10%, 15% and 75% of the total hits respectively. The slight bias towards a negative drift rate is due to non-geosynchronous satellites²¹. The majority of events occur below an S/N threshold of 10^3 because faint signals are less likely to be detected in our shorter reference observations. Stronger signals are also generally associated with nearby ground-based transmitters that will appear in both on-source and off-source observations.

Of the 5,160 events, only one event (Fig. 4) passed all rounds of filtering and visual inspection of dynamic spectra. The event does not lie within the frequency range of any known local radiofrequency interference (RFI), and has many characteristics consistent with a putative transmitter located in another stellar system. This event, which we refer to as a signal of interest, has been previously reported as ‘BLC1’, short for ‘Breakthrough Listen Candidate 1’. We note that ‘signal of interest’ is more appropriate than ‘candidate’²², but for consistency we will adopt BLC1 throughout.

BLC1 was detected at 982.002571 MHz, with a drift rate of 0.038 Hz s^{-1} . The signal of interest was detected over a ~ 2.5 h period, and is only present in pointings towards Prox Cen. According to the US Federal Communications Commission and the Australian Radiofrequency Spectrum Plan, BLC1 lies within a frequency band reserved for aeronautical radionavigation; however, no transmitters that operate at the detected frequency of BLC1 are registered within 1,000 km of the observatory. Radionavigation stations are ground based, so are less likely to be directionally sensitive. It is unlikely that an aircraft or satellite would be present in the direction of Prox

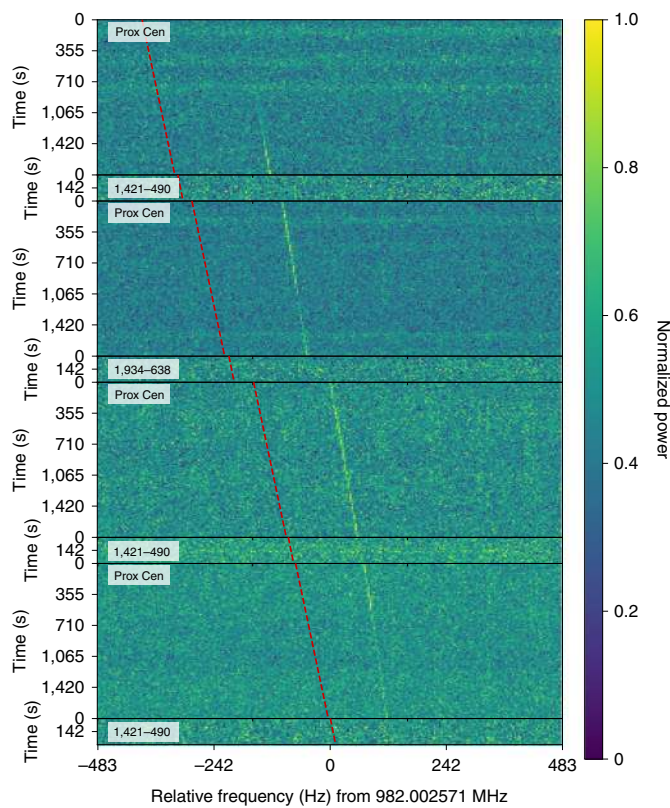


Fig. 4 | The signal of interest, BLC1, from our search of Prox Cen. Here, we plot the dynamic spectrum around the signal of interest over an eight-pointing cadence of on-source and off-source observations. BLC1 passes our coincidence filters and persists for over 2 h. The red dashed line, purposefully offset from the signal, shows the expected frequency based on the detected drift rate (0.038 Hz s^{-1}) and start frequency in the first panel. BLC1 is analysed in detail in a companion paper²³.

Table 1 | Total hits above our thresholds, events that occur in two ONs but no OFFs, and the final candidates that cannot be immediately attributed to RFI

Band	Hits	Events	Candidates
UHF	869,081	2,566	1
L	1,538,111	2,528	0
S	1,952,162	66	0
Parkes UWL	4,172,702	5,160	1

Cen over the course of the signal of interest. BLC1 is analysed in further detail in a companion paper²³. As detailed in the companion paper, we ultimately conclude that BLC1 is a complex inter-modulation product of multiple human-generated interferers: not a technosignature.

Given our non-detection of technosignatures, we place limits on the detection of narrowband signals from Prox Cen by calculating the minimum detectable EIRP ($EIRP_{\min}$). The $EIRP_{\min}$ is given by

$$EIRP_{\min} = 4\pi d^2 F_{\min} \quad (1)$$

where d is the distance to the source (1.301 pc for Prox Cen) and F_{\min} is the minimum detectable flux in watts per square metre. The equation for F_{\min} depends on the minimum S/N (S/N_{\min}), the system temperature of the telescope (T_{sys}), the effective collecting area of the

Table 2 | Parameters used in the Doppler drift rate calculation from equation (3). Data for Prox Cen and Prox Cen b were taken from refs. 38 and 31. Using the listed uncertainties, we calculate maximum drift rate errors of $\dot{\nu}_{\max} = 0.24 \text{ mHz s}^{-1}$ and $\dot{\nu}_{\max} = 1.38 \text{ mHz s}^{-1}$ at 704 MHz and 4,032 MHz respectively

Parameter	Value
R_{pb}	$1.07^{+0.38}_{-0.31} R_{\oplus}$
P_{pb}	$11.18427 \pm 0.00070 \text{ d}$
r_{pb}	$0.04864 \pm 0.00031 \text{ AU}$
M_{pc}	$0.1221 \pm 0.0022 M_{\odot}$

telescope (A_{eff}), the channel bandwidth (B), the number of polarizations (n_{pol}) and the total observation time (t_{obs})^{16,17}:

$$F_{\min} = S/N_{\min} \frac{2k_B T_{\text{sys}}}{A_{\text{eff}}} \sqrt{\frac{B}{n_{\text{pol}} t_{\text{obs}}}} \quad (2)$$

k_B is the Boltzmann constant. We calculate $F_{\min} = 9.2 \text{ Jy Hz}$ and $EIRP_{\min} = 1.9 \text{ GW}$. This $EIRP_{\min}$ is 3.6 times smaller than that previously reported, $EIRP_{\min} = 6.2 \text{ GW}$, for observations of Prox Cen¹⁷. The improved $EIRP_{\min}$ is due to the lower T_{sys} of the ultrawide-bandwidth, low-frequency receiver (UWL) (22 K), compared with the Parkes 10 cm receiver (35 K), and our longer t_{obs} , 5 min versus 30 min. Additionally, our $EIRP_{\min}$ is 1.6 times smaller than Green Bank Telescope L-band (1.1–1.9 GHz) and S-band (1.7–2.6 GHz) observations of the second closest star outside the α Cen system, Barnard's Star (GJ 699). As such, our search of Prox Cen is decisively a very sensitive and comprehensive technosignature search for a stellar target.

On the basis of previous SETI searches and analysis²⁴, it is clear that putative narrowband transmitters are rare. As such, it is statistically probable that any signal of interest is a pathological case of human-generated interference. Extended and rigorous analysis of BLC1 was required to ascertain its progeny; this is presented in the companion paper²³, alongside a framework for verification of future signals of interest.

Alone, this search—or more generally any band-limited single-target search—cannot disprove the existence of a technologically advanced society on Prox Cen b. While the UWL receiver has a wide bandwidth, we have still not covered the entire radio spectrum, nor optical, infrared or X-ray bands. In addition to false positives, RFI could also confound detection of technosignatures at coincident frequencies. Prox Cen remains an interesting target for technosignature searches, and we encourage continued observations with other facilities and alternative approaches.

Methods

For the observations of Prox Cen presented here, we used the Parkes UWL²⁵. The receiver has an effective T_{sys} of 22 K and system equivalent flux density of 28 Jy across ~60% of the band. The UWL receiver covers a 3.3 GHz wide bandwidth from 0.704 to 4.032 GHz.

Observations were conducted from UT 2019 April 29 to UT 2019 May 4, as part of the P1018 project 'Wide-band radio monitoring of space weather on Prox Cen. In this project, Parkes observations were part of a multiwavelength campaign in which Prox Cen was monitored for stellar flare activity'. Observations were conducted using the BL Parkes digital recorder^{26,27} (BLPDR) in parallel with the primary UWL digital signal processor, 'Medusa'. For the purposes of a narrowband technosignature search, we deal solely with Stokes I data from BLPDR. For the purposes of detecting flare activity, data from Medusa—which was configured to produce a full-Stokes data product at high time resolution (128 μs) but low frequency resolution (1 MHz)—were also recorded; however, these data are not included in our analysis given their relative insensitivity to narrowband signals.

Observation strategy. Over the period UT 2019 April 29 to UT 2019 May 4, we observed Prox Cen for a total of 26h 9min. The observations were conducted as

a series of on-source, off-source pointings (a ‘cadence’) to enable rejection of RFI, similar to previous BL observations^{16,17}. The on-source pointings (A) were towards Prox Cen (14h 29m 42.95s, $-61^{\circ}59'53.84''$) while the off-source pointings (B) were primarily the calibrator source PKS 1421-490 (14h 24m 32.24s, $-49^{\circ}26'50.26''$) with the exception of two of the pointings, which used PKS 1934-638 (19h 39m 25.03s, $-62^{\circ}57'54.34''$), a well characterized flux calibrator for Parkes.

Our observations differed from standard BL searches in two ways. First, our observation lengths were ~ 30 min on source and ~ 5 min off source; previous BL searches^{16,17} employed a 5 min on-source, 5 min off-source observation style. A longer observation time was chosen to maximize time on Prox Cen to search for flare emission: a key element, which may determine the habitability of Prox Cen b. Longer observations mean we are insensitive to signals lasting less than 30 min because we do not have intervening off-source pointings needed to discern if a hit is caused by RFI. However, we are sensitive to signals that are broadcast over a long period of time (an hour or longer) because we can see how that signal changes over time (for example, drift rate changes). We are also more sensitive to weaker signals because we can integrate over the whole 30 min observation to look for a persistent signal.

Second, we used longer cadences—sets of pointings towards the target source and reference sources—than the six-pointing default for BL. The total number of pointings in a single observation ranged from 12 to 17. This gives us the flexibility to choose a subset of cadences from a larger number of pointings per day. In our initial search, we considered four-pointing cadences, meaning, for example, that if an observation consisted of 12 pointings we looked at nine subset cadences in that observation.

Data format. Data are processed using a pipeline run on the BLPDR. BLPDR provides data in 26 separate files, each containing a 128 MHz subband from the 0.7–4.0 GHz band. The high-spectral-resolution products, as used here for detection of artificial narrowband signals, have a frequency resolution of ~ 3.81 Hz (that is, 2²⁵ channels across each 128 MHz band) and time integrations of ~ 16.78 s. The final data product is stored in filterbank format, which can then be opened by the Blimp Python package²⁸. The final data volume for the 6 d observation period is 19.5 TB: about 118 times more data than were obtained for any single source in previous BL searches¹⁷.

The Python/Cython package turboSETI²⁹ is used to search over a range of drift rates in the data. Reference¹⁶ describes how the program works in greater detail. Two important parameters required by turboSETI are a minimum S/N, and a maximum possible drift rate. The minimum S/N was set to 10, following previous work¹⁷. However, we tailored the drift rate range to the specific characteristics of Prox Cen b’s rotation and orbit.

Expected drift rate. The most dominant factors affecting the drift rate of a signal are the rotations and orbits of the Earth and the source body. The following equation³⁰ gives us the maximum expected Doppler drift rate ($\dot{\nu}_{\max}$) by accounting for planet rotation ($\frac{4\pi^2 R}{P_{\oplus}}$) and orbit ($\frac{GM}{r}$):

$$\dot{\nu}_{\max} = \frac{\nu_0}{c} \left(\frac{4\pi^2 R_{\oplus}}{P_{\oplus}^2} + \frac{4\pi^2 R_{\text{Pb}}}{P_{\text{Pb}}^2} + \frac{GM_{\odot}}{r_{\oplus}^2} + \frac{GM_{\text{PC}}}{r_{\text{Pb}}^2} \right). \quad (3)$$

The term ν_0 is the emitted frequency from the transmitter; R , P , M and r are the planetary radii, rotational periods, solar masses and orbital radii for Earth, Prox Cen b (subscript Pb) the Sun and Prox Cen (subscript PC), respectively. Other contributions to the drift rate, such as the bodies’ movement through the Milky Way, are negligible.

To limit computation time, an initial search of ± 3 Hz s⁻¹ was performed across all frequencies. However, we expect $\dot{\nu}_{\max} = 4.191$ Hz s⁻¹ at 4,000 MHz using the parameters from Table 2 and equation (3). Therefore, a supplementary search over ± 4 Hz s⁻¹ from 2,752 to 3,648 MHz and ± 5 Hz s⁻¹ from 3,648 to 4,032 MHz was necessary to search the complete range of possible drift rates expected. Nevertheless, putative transmitters orbiting Prox Cen b could exhibit drift rates orders of magnitude higher³⁰; extending to such high drift rates is computationally challenging, and we do not consider these here.

Finding events. To find candidate events, we run the hits (signals above the S/N threshold) found by turboSETI through a secondary pipeline, which compares on-source and off-source pointings. We classify an event as any narrowband hit that exists in an on-source pointing, but not any of the off-source observations. Typical BL SETI searches with single-dish telescopes use a cadence length of six (ABABAB, three on-source and three off-source observations); however, we use a cadence length of four (ABAB) due to our longer observation times. A shorter cadence relaxes the requirement that events are detected in all on-source observations; that is, we allow events with ~ 1 h duration. Once an event is found in a cadence of four, we search additional pointings to see if it occurs over a longer time period. Note that cadences are primarily used as a discriminant for RFI; as the narrowband search is run separately on each pointing, longer cadences do not increase sensitivity.

Filtering events. After events that occur in a four-pointing cadence (ABAB) are found, we generate plots that have an additional two pointings to make a

six-pointing cadence (ABABAB). A longer cadence allows visual inspection of the additional pointings for low-S/N hits. For example, an intermittent signal may be present in only the on-source pointings for the four pointings that were searched, but then be present in a successive off-source pointing (Supplementary Fig. 1). We discard events that are clearly present in the off-source observations but are not detected by the search pipeline (that is, the event is present in a successive off-source pointing, but did not meet the S/N threshold of 10, or the drift rate threshold¹⁷).

After an initial list of promising events with a six-pointing cadence is found, we plot cadences of length 12. This longer cadence allows us to see the entire duration of the event and if it occurs in any off-source observations. If an event is present in any off-source observations, it is discarded as local RFI (Supplementary Fig. 2). During this step we also discard events that share similar characteristics (drift rate, frequency or profile) with other hits that are found in off-source observations. Finally, any candidate event that lies in the frequency range of nearby registered ground or satellite transmitters is marked as suspicious (Supplementary Fig. 3).

Every event that passes the two rounds of visual inspection and lies within no registered transmitters is scrutinized. Extensive research is done on the frequency bands within which the event lies. We use allocation charts such as the ARSP (Australian Radiofrequency Spectrum Plan), which contains an extensive list of the types of transmitter allocated to specific frequency bands, and the Australian Communications and Media Authority Register of Radiocommunications Licences (<https://web.acma.gov.au/rri/>).

Data availability

The data used in this work are available for download via <https://seti.berkeley.edu/blc1>. Correspondence and requests for other materials should be addressed to D.C.P.

Code availability

Data analysis was performed using the Blimp²⁸ and turboSETI²⁹ Python packages. These codes are open source and are available from <https://github.com/UCBerkeleySETI/> and the Python Package Index (<https://pypi.org/>)³². The Blimp and turboSETI packages make use of Astropy^{33,34}, h5py³⁵, Matplotlib³⁶, NumPy³⁷ and Pandas³⁸.

Received: 5 March 2021; Accepted: 4 August 2021;

Published online: 25 October 2021

References

1. Anglada-Escudé, G. et al. A terrestrial planet candidate in a temperate orbit around Proxima Centauri. *Nature* **536**, 437–440 (2016).
2. Ribas, I. et al. The habitability of Proxima Centauri b. I. Irradiation, rotation and volatile inventory from formation to the present. *Astron. Astrophys.* **596**, A111 (2016).
3. Turbet, M. et al. The habitability of Proxima Centauri b. II. Possible climates and observability. *Astron. Astrophys.* **596**, A112 (2016).
4. Alvarado-Gómez, J. D. et al. An earth-like stellar wind environment for Proxima Centauri c. *Astrophys. J. Lett.* **902**, L9 (2020).
5. Howard, W. S. et al. The first naked-eye superflare detected from Proxima Centauri. *Astrophys. J. Lett.* **860**, L30 (2018).
6. Zic, A. et al. A flare-type IV burst event from Proxima Centauri and implications for space weather. *Astrophys. J.* **905**, 23 (2020).
7. MacGregor, M. A. et al. Discovery of an extremely short duration flare from Proxima Centauri using millimeter through far-ultraviolet observations. *Astrophys. J. Lett.* **911**, L25 (2021).
8. Tarter, J. C. et al. A reappraisal of the habitability of planets around M dwarf stars. *Astrobiology* **7**, 30–65 (2007).
9. Parkin, K. L. G. The Breakthrough Starshot system model. *Acta Astronaut.* **152**, 370–384 (2018).
10. Backus, P. R. Project Phoenix SETI observations at Parkes. In *Proc. American Astronomical Society Meeting* 41.01 (AAS, 1995).
11. Tarter, J. C. Project Phoenix: the Australian deployment. *Proc. SPIE* **2704**, 24–34 (1996).
12. Blair, D. G. et al. A narrow-band search for extraterrestrial intelligence (SETI) using the interstellar contact channel hypothesis. *Mon. Not. R. Astron. Soc.* **257**, 105–109 (1992).
13. Marcy, G. W. A search for optical laser emission from Proxima Centauri. *Mon. Not. R. Astron. Soc.* **505**, 3537–3548 (2021).
14. Worden, S. P. et al. Breakthrough Listen—a new search for life in the universe. *Acta Astronaut.* **139**, 98–101 (2017).
15. Isaacson, H. et al. The Breakthrough Listen search for intelligent life: target selection of nearby stars and galaxies. *Publ. Astron. Soc. Pac.* **129**, 054501 (2017).
16. Enriquez, J. E. et al. The Breakthrough Listen search for intelligent life: 1.1–1.9 GHz observations of 692 nearby stars. *Astrophys. J.* **849**, 104 (2017).
17. Price, D. C. et al. The Breakthrough Listen search for intelligent life: observations of 1327 nearby stars over 1.10–3.45 GHz. *Astron. J.* **159**, 86 (2020).
18. Sheikh, S. Z. et al. The Breakthrough Listen search for intelligent life: a 3.95–8.00 GHz search for radio technosignatures in the restricted earth transit zone. *Astron. J.* **160**, 29 (2020).

19. Traas, R. et al. The Breakthrough Listen search for intelligent life: searching for technosignatures in observations of TESS targets of interest. *Astron. J.* **161**, 286 (2021).
20. Gajjar, V. et al. The Breakthrough Listen search for intelligent life near the Galactic Center. I. *Astron. J.* **162**, 33 (2021).
21. Zhang, J., Zhang, K., Grenfell, R. & Deakin, R. GPS satellite velocity and acceleration determination using the broadcast ephemeris. *J. Navig.* **59**, 293–305 (2006).
22. Forgan, D. et al. Rio 2.0: revising the Rio scale for SETI detections. *Int. J. Astrobiol.* **18**, 336–344 (2019).
23. Sheikh, S. Z. et al. Analysis of the Breakthrough Listen signal of interest blc1 with a technosignature verification framework. *Nat. Astron.* <https://doi.org/10.1038/s41550-021-01508-8> (2021).
24. Włodarczyk-Sroka, B. S., Garrett, M. A. & Siemion, A. P. V. Extending the Breakthrough Listen nearby star survey to other stellar objects in the field. *Mon. Not. R. Astron. Soc.* **498**, 5720–5729 (2020).
25. Hobbs, G. et al. An ultra-wide bandwidth (704 to 4032 MHz) receiver for the Parkes radio telescope. *Publ. Astron. Soc. Aust.* **37**, e012 (2020).
26. Price, D. C. et al. The Breakthrough Listen search for intelligent life: wide-bandwidth digital instrumentation for the CSIRO Parkes 64-m telescope. *Publ. Astron. Soc. Aust.* **35**, 41 (2018).
27. Price, D. C. et al. Expanded capability of the Breakthrough Listen Parkes Data Recorder for observations with the UWL receiver. *Res. Notes Am. Astron. Soc.* **5**, 114 (2021).
28. Price, D., Enriquez, J., Chen, Y. & Siebert, M. Blimp: Breakthrough Listen I/O Methods for Python. *J. Open Source Softw.* **4**, 1554 (2019).
29. Enriquez, E. & Price, D. turboSETI: Python-based SETI search algorithm. *Astrophysics Source Code Library* ascl:1906.006 (2019).
30. Sheikh, S. Z., Wright, J. T., Siemion, A. & Enriquez, J. E. Choosing a maximum drift rate in a SETI search: astrophysical considerations. *Astrophys. J.* **884**, 14 (2019).
31. Suárez Mascareño, A. et al. Revisiting Proxima with ESPRESSO. *Astron. Astrophys.* **639**, A77 (2020).
32. Astropy Collaboration et al. Astropy: a community Python package for astronomy. *Astron. Astrophys.* **558**, A33 (2013).
33. Astropy Collaboration et al. The Astropy Project: building an open-science project and status of the v2.0 core package. *Astron. J.* **156**, 123 (2018).
34. Collette, A. *Python and HDF5* (O'Reilly, 2013).
35. Hunter, J. D. Matplotlib: a 2D graphics environment. *Comput. Sci. Eng.* **9**, 90–95 (2007).
36. Harris, C. R. et al. Array programming with NumPy. *Nature* **585**, 357–362 (2020).
37. McKinney, W. Data structures for statistical computing in Python. In *Proc. Ninth Python in Science Conference* (eds van der Walt, S. & Millman, J.) 56–61 (2010).
38. Bixel, A. & Apai, D. Probabilistic constraints on the mass and composition of Proxima b. *Astrophys. J. Lett.* **836**, L31 (2017).

Acknowledgements

BL is managed by the Breakthrough Initiatives, sponsored by the Breakthrough Prize Foundation. The Parkes radio telescope is part of the Australia Telescope National Facility, which is funded by the Australian Government for operation as a National Facility managed by CSIRO. S.S. and S.C. were supported by the National Science Foundation under the Berkeley SETI Research Center REU site grant 1950897.

Author contributions

S.S. and D.C.P. led the data analysis and are primary authors of the manuscript. S.Z.S. led in-depth analysis of BLC1. D.J.C., S.C., D.D., V.G., H.I., B.C.L., C.N., K.I.P., A.P.V.S. and C.I.W. assisted with interpretation, manuscript preparation and revision, and data analysis. M.L. and D.H.E.M. provided instrument support, managed data and aided observations. A.Z. was lead observer during Parkes observations and aided manuscript preparation. J.D. and S.P.W. aided manuscript preparation and provided logistical support.

Competing interests

The authors declare no competing interests.

Additional information

Supplementary information The online version contains supplementary material available at <https://doi.org/10.1038/s41550-021-01479-w>.

Correspondence and requests for materials should be addressed to Danny C. Price.

Peer review information *Nature Astronomy* thanks Chenoa Tremblay and the other, anonymous, reviewer(s) for their contribution to the peer review of this work.

Reprints and permissions information is available at www.nature.com/reprints.

Publisher's note Springer Nature remains neutral with regard to jurisdictional claims in published maps and institutional affiliations.



Open Access This article is licensed under a Creative Commons Attribution 4.0 International License, which permits use, sharing, adaptation, distribution and reproduction in any medium or format, as long as you give appropriate credit to the original author(s) and the source, provide a link to the Creative Commons license, and indicate if changes were made. The images or other third party material in this article are included in the article's Creative Commons license, unless indicated otherwise in a credit line to the material. If material is not included in the article's Creative Commons license and your intended use is not permitted by statutory regulation or exceeds the permitted use, you will need to obtain permission directly from the copyright holder. To view a copy of this license, visit <http://creativecommons.org/licenses/by/4.0/>.

© The Author(s) 2021